The results and developments of the radon monitoring network in seismic areas

Victorin Emilian TOADER *, Constantin Ionescu, Iren-Adelina Moldovan, Alexandru Marmureanu, Nicoleta-Sanda Brisan, Iosif Lıngvay, Andrei Mihai

Posted Date: 23 May 2023

doi: 10.20944/preprints202305.1645.v1

Keywords: radon and CO2 monitoring; anomaly detection; multidisciplinary monitoring; precursor phenomena; air ionization monitoring; OEF (Operational Earthquake Forecasting).

Article

The Results and Developments of the Radon Monitoring Network in Seismic Areas

Victorin-Emilian Toader [1,*], Constantin Ionescu [1], Iren-Adelina Moldovan [1], Alexandru Marmureanu [1], Nicoleta – Sanda Brisan [2], Iosif Lıngvay [3] and Andrei Mihai [1]

[1] National Institute for Earth Physics, Calugareni 12, RO077125 Magurele, Romania; victorin@infp.ro (V.-E.T.); viorel@infp.ro (C.I.); iren@infp.ro (I.-A.M.); marmura@infp.ro (A.M.)
[2] Faculty of Environmental Science and Engineering, Babeş-Bolyai University, Cluj-Napoca, Romania, nicoleta.brisan@ubbcluj.ro (N.B.-B.)
[3] S.C. Electrovâlcea SRL Râmnicu Vâlcea, str. Ferdinand 19, Romania, iosiflingvay@yahoo.com (I.L)
* Correspondence: victorin@infp.ro

Abstract: The analysis of the radon-seismicity relationship has been carried out so far in the Vrancea (Romania) seismic zone, with monitoring stations positioned on tectonic faults. The article analyzes the evolution of radon under the conditions of the existence of deep and surface seismicity and the presence of mud volcanoes along with live fires caused by gases emitted from the soil. The monitoring area was extended to the Black Sea and the area of the Făgăraș Câmpulung fault, where a special radon detection system was set up, which was proposed for patenting. A case study is the effect of the earthquakes in Turkey (7.8 R and 7.5 R on 2023/02/06) on the seismically active areas in Romania in terms of gas emissions (radon, CO_2). The main analysis methods on radon (we also included CO_2) are applied to integrated time series and the use of anomaly detection algorithms. Data analysis shows that the effects of global warming introduce deviations in seasonal gas emissions compared to previous years. This makes it difficult to analyze the data and correlate them with seismicity. The main conclusions related to the development of a radon monitoring network and in general the emission of gases in seismic areas refer to the importance of the choice of equipment, the monitoring location and the installation method.

Keywords: radon and CO_2 monitoring; anomaly detection; multidisciplinary monitoring; precursor phenomena; air ionization monitoring; OEF (Operational Earthquake Forecasting)

1. Introduction

This article presents the evolution of implementations and results from the development process of a radon monitoring network as part of a multidisciplinary approach by the National Institute of Earth Physics in Romania ([1–3]). The main goal is to create an automated seismic forecasting system (OEF - Operational Earthquake Forecasting) based on real-time data such as radon, CO_2, air ionization, telluric currents, magnetic field, ULF - VLF radio waves and seismic information. Realizations of this type exist each following a certain parameter for detection ([4–9]) but each solution refers to a certain area that is monitored. In [3] and [5] an application for the Vrancea zone (the curvature area of the Carpathian Mountains) are presented, in [4] the forecasting is for Japan, [6] use a general monitoring of electromagnetic emissions (EM) (we tried something similar but the results are not convincing for Vrancea [10]), and [7] prospects for operational forecasting of earthquakes in Europe using seismic information, but the catalogs are not homogeneous and the seismicity patterns are too different for different areas. The authors of the article [8] specify the difference between forecast and prediction, emphasizing the difficulties of using it in general the 'time-dependent seismic hazards to help communities prepare for potentially destructive earthquakes'. The main problem of using seismic catalogs is that they reflect more the detection capacity of the respective networks. The most recent example for Romania is OLTENIA, GORJ area

 doi:10.20944/preprints202305.1645.v1

where more than 2000 surface earthquakes occurred recently and which was reclassified as a seismic risk area after 200 years (Table 7, https://data.mendeley.com/datasets/ds4hwchkp7/1). The large number of earthquakes is due to the increase in detection capacity as a result of monitoring with a larger number of seismic stations installed in that area. Even if the statistical methods are correct, they are applied on insufficient data, especially when they refer to natural phenomena. Radon monitoring also expanded as a result of the development of monitoring equipment, which depended on technological development in general. Our efforts to integrate real-time radon data were described in [3]. At the current stage, all multidisciplinary information is accessible in real time from a database that has an interface for viewing at gebs.infp.ro (API interface - JSON format, sample data at https://data.mendeley.com/datasets/28kv3gsgcz/2). The biggest challenges were the integration of data coming from equipment with different hardware and software interface options, the creation of metadata, the implementation of the database, its management and access to information. Radon concentration as seismic precursor is mention into OEF [9] along the fluctuations of the 'groundwater level, electromagnetic variations near and above the Earth's surface, thermal anomalies, abnormal animal behavior, seismicity models' and with the possibility of generating false alarms.

In this paper we analyze the relationship between radon and CO_2 emissions with seismicity and meteorological conditions, along with several case studies such as the relationship between the recent seismic events in Turkey (7.8 R, Figure 4, and Table 6) and seismicity in Romania, or exceeding the radon level in a few situations. A description of the network (stations, equipment, their positioning, activity periods, measurement results) and metadata is made in Chapter 2. A special case is represented by the Râmnicu Vâlcea station, which is built to monitor radon (patent application [11]). The analysis methods used are described in [2,3] and are applied to several case studies. The first refers to the use of radon and CO_2 in the correlation of seismic events in Turkey (7.8R) and those in the Râmnicu Sărat area (Romania), followed by the analysis of an earthquake sequence from Vrancea with a magnitude of 4.2R through the prism of gas emissions, a case of pollution at Black Sea caught in the attempt to monitor the Shabla area and exceeding the level of 300 Bq/mc (the limit established by Council Directive 2013/59/EURATOM) in several situations. We also performed an analysis of the dependence of radon and CO2 emissions on meteorological factors, seismic energy and the seismicity of Vrancea represented by the parameters a-b from the Gutenberg-Richter law [12,13]. In these cases, we used correlation and averaging functions on sliding time windows applied to radon time series. The results are relative to the function-based methods in the LabVIEW programming environment library. An aspect analyzed is the correlation of the radon emission with the specifics of the Vrancea area, which is characterized by intermediate earthquakes (unlikely to directly generate gas emissions) as well as crustal ones. Finally, the analysis of data starting with 2016 shows that climate changes have the effect of increasing radon emissions along with temperature.

2. The new Radon and CO_2 Monitoring Network

The first development of a radon detection equipment for Vrancea was carried out by IFIN HH and was installed in the Plostina station (INFOSOC 2006 project - Complex system for monitoring and processing through modern techniques precursor factors of major seismic events, Figure 1). The high radon values in Figure 1 were not confirmed by the measurements made with a RADON SCOUT type equipment installed in 2017 in the same location and which is still working today (Table 1).

Preprints (www.preprints.org) | NOT PEER-REVIEWED | Posted: 23 May 2023 doi:10.20944/preprints202305.1645.v1

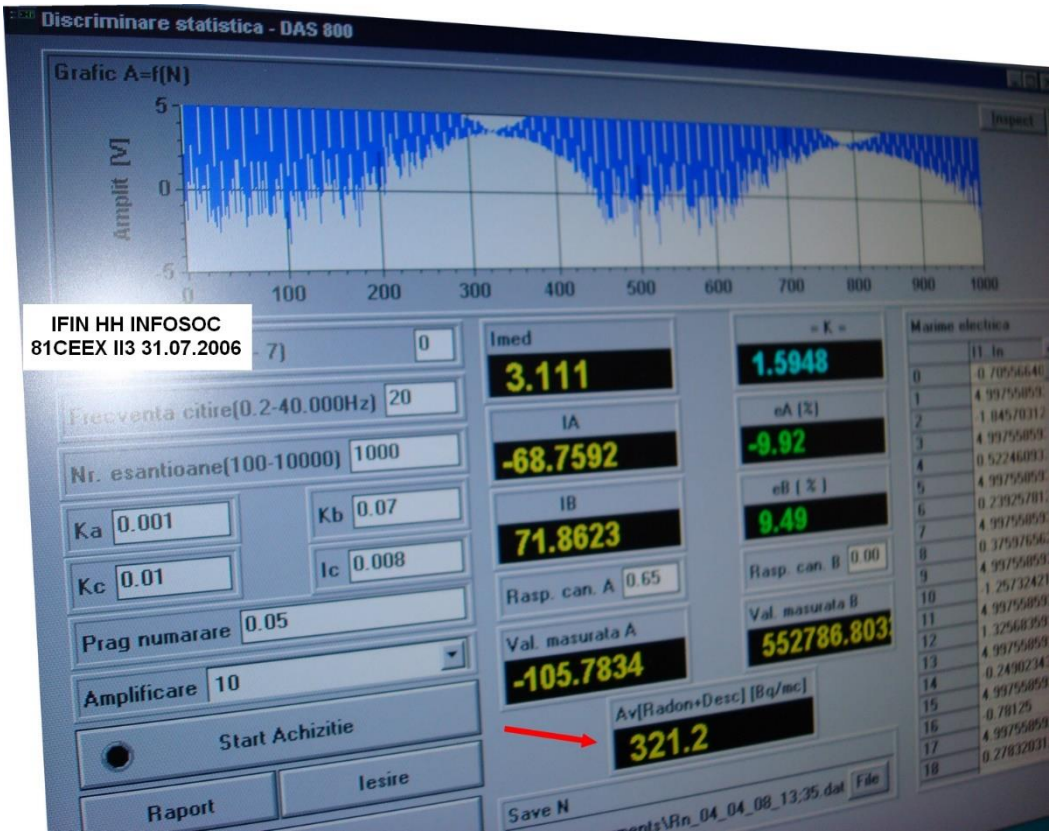

Figure 1. The first development of experimental radon detection equipment in a seismic zone was carried out by IFIN HH, 2006.

Table 1. Radon network, locations, equipment, period of operation.

Station	Location	Equipment	North	East	Description	Start	End
agigea	Agigea	RADONSCOUT	44.0838	28.6412	Agigea, radon	14/08/31	14/09/05
chiurus	Chiurus	RADONSCOUT	45.8233	26.1646	Chiurus, radon	14/09/18	14/09/18
INFPr	Magurele	RADONSCOUT	44.3479	26.0281	INFP radon	14/09/12	14/09/15
MLRdd	Muntele Rosu	RADONSCOUT	45.4909	25.9450	MLR, radon	15/11/02	17/03/22
ODBIdd	Odobesti	RADONSCOUT	45.7633	27.0558	Odbi, radon	14/10/24	15/08/04
PLRdd1	Plostina 4	RADONSCOUT	45.8512	26.6498	PLOR1, radon	17/08/01	17/11/28
PLRdd2	Plostina 4	RADONSCOUT	45.8512	26.6498	PLOR1, radon	17/11/28	_
BISRdd	Bisoca	RADONSCOUTp	45.5481	26.7099	Bisc, radon	14/10/22	21/05/20
BISRAERd	Bisoca	AERC	45.5481	26.7099	Biscoca, radon	21/02/25	
DLMdd	Dalma	RADONSCOUTp	45.3629	26.5965	Dalma, radon	22/07/04	_
LOPRdd	Lopatari	RADONSCOUTp	45.4738	26.5680	Mocearu, radon	15/08/06	_
MNGdd	Mangalia	RADONSCOUTp	43.8168	28.5876	Mangalia, radon	21/10/20	22/04/14
NEHRdd	Nehoiu	RADONSCOUTp	45.4272	26.2952	NEHR, radon	15/08/06	_
PANCdd	Panciu	RADONSCOUTp	45.8723	27.1477	PANC, radon	21/09/29	_
RMGVdd	Râmnicu Vâlcea	RADONSCOUTp	45.1075	24.3770	Electrovalcea, radon	20/08/22	_
SAHRdd	Sahastru	RADONSCOUTp	45.7266	26.6854	SAHR, radon	21/05/20	_
SURLdd	Surlari	RADONSCOUTp	44.6777	26.2526	Surlari, radon	21/11/10	_
VRIdd	Vrancioaia	RADONSCOUTp	45.8657	26.7277	Vri, radon	14/10/23	20/07/21

Concerns related to the correlation of radon emission and seismicity have expanded and materialized in a multidisciplinary monitoring network that currently also includes gas emission as

Preprints (www.preprints.org) | NOT PEER-REVIEWED | Posted: 23 May 2023 doi:10.20944/preprints202305.1645.v1

a precursor parameter ([2,3]). In Figure 2 (the green place marks indicate radon and CO_2, yellow mean only radon equipment) and Table 1 presents the development of the radon monitoring network to which CO_2 was added as a seismic precursor ([14,15]) but also as a parameter used in the analysis of the effects of greenhouse gases and climate change.

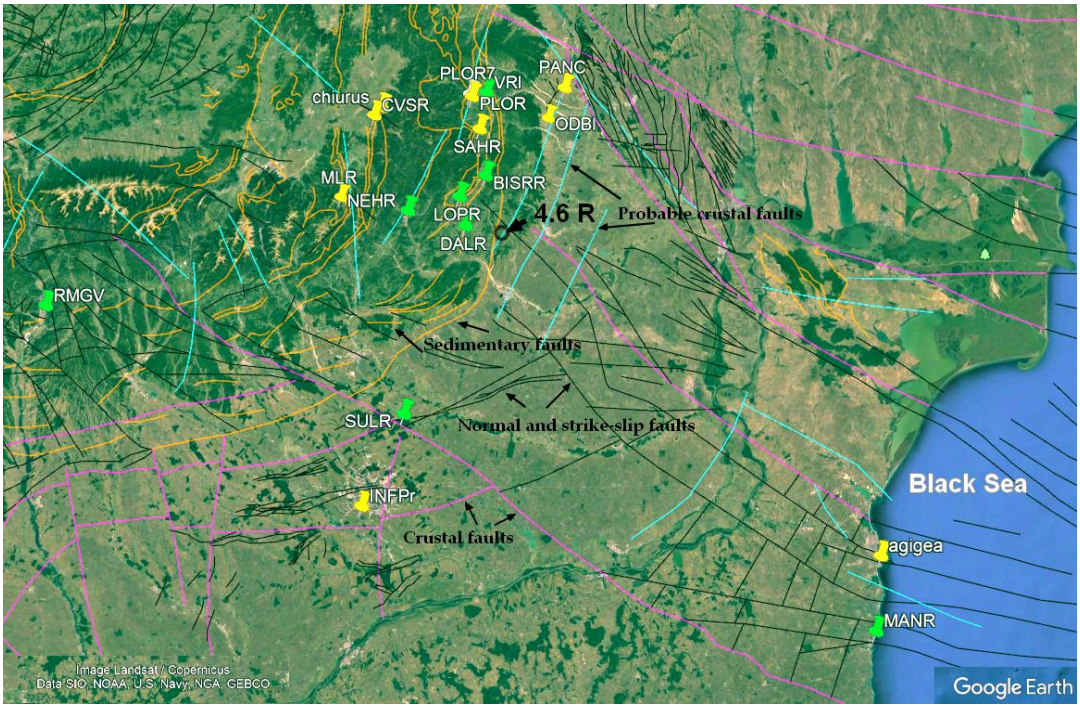

Figure 2. Map of radon and CO_2 monitoring locations.

The monitoring stations are located near the faults (Figure 2), considering that the gas emission is more obvious ([16–19]).

Table 2 shows the results of radon monitoring including Standard Deviation (SD) reference parameters and air temperature. The equipment that determines the level of radon also includes sensors for temperature, humidity and atmospheric pressure, that is, the parameters on which the emission of gases depends ([20,21]).

Table 2. Synthesized results of radon monitoring, the 2SD reference parameter and its dependence on temperature.

Station	Mean Bq/mc	2SD	Max Bq/mc	Radon - Max Time (year/month/day)	Mean T(C)	Max/ Min T(C)	Time Interval (year/month/day)	
BISRAERd	70.1835	104.1120	500.0	2020/09/28	17.0133	29.0/-1.5	20/01/01	20/12/31
BISRAERd	55.4286	86.2253	498.0	2021/09/21	15.5043	29.0/+1.5	21/01/01	21/12/31
BISRAERd	74.3684	114.6245	432.0	2022/08/04	16.1838	29.0/ -0.5	22/01/01	22/12/31
DLMdd	50.1785	82.1935	321.0	2022/10/18	15.1580	26.5/ +1.0	22/07/04	23/03/12
LOPRdd	9.5060	14.3086	51.0	2020/10/02	16.9339	39.5/-3.0	20/01/01	20/12/31
LOPRdd	8.6471	12.3745	40.0	2021/06/26	16.2484	43.5/ -1.0	21/01/01	21/12/31
LOPRdd	9.1671	15.1524	71.0	2022/05/17	14.7775	36.5/-1.0	22/01/01	22/12/31
PLRdd2	54.0582	66.8106	607.0	2020/06/18	11.5113	26.5/-1.0	20/01/01	20/12/31
PLRdd2	51.3739	84.3485	1068.0	2021/12/12	10.4853	26.5/-2.5	21/01/01	21/12/31
PLRdd2	57.0862	135.1785	1077.0	2022/09/04, 2022/09/05	11.2713	26.5/-1.0	22/01/01	22/12/31
MLRdd	518.3502	1090.3606	3230.0	2016/07/20	7.0435	8.5/+5.5	16/01/01	16/12/31

Preprints (www.preprints.org) | NOT PEER-REVIEWED | Posted: 23 May 2023 doi:10.20944/preprints202305.1645.v1

NEHRdd	17.1800	22.7589	75.0	2020/12/08	16.7921	37.5/-0.5	20/01/01	20/12/31
NEHRdd	17.9657	24.0877	71.0	2021/10/15	15.5227	36.5/-0.5	21/01/01	21/12/31
NEHRdd	18.0120	23.9987	71.0	2022/09/09	16.1370	38.5/-4.5	22/01/01	22/12/31
PANCdd	73.5889	216.1618	681.0	2022/12/10	13.2224	35.5/-7.0	22/01/01	22/12/31
RMGVdd	25.1879	26.0728	122.0	2021/06/18	12.3352	35.0/-6.5	21/10/20	22/04/14
RMGVdd	28.0030	25.2148	90.0000	2022/08/16, 2022/11/17	12.8718	35.0/-7.0	22/01/01	22/12/31
SAHRdd	87.4349	137.4242	413.0000	2022/07/29, 2022/08/18	20.4269	41.0/+2.5	22/01/01	22/12/31
SURLdd	316.9367	320.4041	1095.0000	2022/12/07	13.8398	28.0/-1.5	22/01/01	22/12/31
VRIdd	148.8226	157.1080	413.0000	2018/01/25	14.7503	26.0/-3.0	18/01/01	18/12/31
VRIdd	165.6702	219.5496	622.0000	2019/12/05	15.7668	29.5/+0.5	19/01/01	19/12/31
VRIdd	202.7971	240.1850	642.0000	2020/01/07	15.3096	28.5/+3.0	20/01/01	20/07/21
agigea	55.3043	51.5058	115.0000	2014/09/01	21.2522	22.5/21.0	14/08/31	14/09/05
MNGdd	313.7032	451.5302	1163.0000	2021/12/02	10.1699	25.0/-3.0	21/10/20	22/04/14

In most cases, the radon anomaly is defined as the positive deviation that exceeds the average radon level by more than two Standard Deviation, 2SD ([22–24]). The temperature T(C) in the Table 2 is measured by the equipment that determines the level of radon. We observe that radon level is over 300 Bq/mc (the limit established by Council Directive 2013/59/EURATOM of December 5, 2013) in MLRdd, SURLdd, and MNGdd. In the first case, the measurements were made in a tunnel in the mountain, which explains the high values. The limit values determined in Surlari (SURLdd) can be explained by the effect of the forest in which the monitoring location is located. In the last case (a case study will follow), Mangalia MNGdd, we recorded very high values and variations of radon, CO_2 and CO (Figure 8). There is a proportional relationship between the radon level and the temperature in the case of the stations BISRAERd, PLRdd2, and RMGVdd (Table 2.). In the other stations, this relationship is not preserved, which means that the temperature is not a determining factor in the evolution of the radon level, which depends a lot on the local conditions in which the equipment is installe ([25]). The fluctuations that occur are caused by the fact that radon can be brought by the wind from other areas compared to the case of the BISRAERd, PLRdd2, and RMGVdd stations where the spaces where the measurements are made are more isolated.

Radon variations are not sufficient to implement a seismic forecasting method. Other types of equipment are also installed in all monitoring stations. Table 3 shows some of them (CO_2 and weather stations) that contribute, along with radon, to the analysis of seismic precursors. An example of the analysis of the relationship between radon and CO_2 is in the article [26].

Table 3. Equipment that is part of the multidisciplinary monitoring of seismic areas.

Station	Location	Equipment	North	East	Per (sec)	Description	Start	End
MLRttu	Muntele Rosu	DL100	45.4909	25.945	1	Tunnel MLR temperature and humidity	19/11/05	_
LOPrCO2	Lopatari	DL303	45.4738	26.568	1	Lopatari Mocearu CO_2/CO	19/06/26	_
VRIco2	Vrancioaia	DL303	45.8657	26.7277	1	Vrancioaia CO_2/CO	19/07/10	20/07/21

Preprints (www.preprints.org) | NOT PEER-REVIEWED | Posted: 23 May 2023 doi:10.20944/preprints202305.1645.v1

DLMCO2	Dalma	DL303	45.3629	26.5965	1	Dalma CO_2/CO	22/07/04	_
SurlCO2	Surlari	DL303	44.6777	26.2526	1	Surlari CO_2/CO	21/11/10	_
CVSrCO2	Covasna	DL303	45.7944	26.1239	1	Covasna CO_2/CO	22/07/06	_
RVCO2	Râmnicu Vâlcea	DL303	45.1075	24.3770	1	Râmnicu Vâlcea borehole CO_2/CO	21/08/18	22/04/13
PL7co2	Plostina 7	DL303	45.8603	26.6405	1	PLOR7 CO_2/CO	20/07/21	_
MNGCO2	Mangalia	DL303	43.8168	28.5876	1	Mangalia CO_2/CO	21/10/20	22/03/09
BISRCO2	Bisoca	DL303	45.5481	26.7099	1	Bisoca CO_2/CO	19/07/09	_
PL7S	Plostina 7	PL7S	45.8603	26.6405	1	PLOR7 solar radiation, K2	19/11/14	_
BURmto	Bucovina	VANTAGE_PRO2p	47.644	25.2002	60	Bucovina Meteo Vantage	18/10/31	_
EFORmt2	Eforie Nord	VANTAGE_PRO2p	44.075	28.6323	60	Eforie Meteo Vantage Pro2	18/08/02	_
INFPmt2	Magurele	VANTAGE_PRO2p	44.3479	26.0281	60	INFP Magurele Meteo DAVIS Vantage Pro2	18/07/12	_
MetMr2	Marisel	VANTAGE_PRO2p	46.676	23.1189	60	Meteo Davis Marisel	18/07/20	_
MLRmt2	Muntele Rosu	VANTAGE_PRO2p	45.4909	25.945	60	MLR Meteo DAVIS PRO2+	19/11/15	_
VRImto	Vrancioaia	WS2355	45.8657	26.7277	60	VRI Meteo, La Crosse 2.0	14/02/07	_
BISRmto	Bisoca	WS2355	45.5481	26.7099	60	Bisoca, Meteo La Crosse 2.0	17/07/25	_
NEHRmto	Nehoiu	WS2355	45.4272	26.2952	60	Nehoiu, Meteo La Crosse 20	14/05/28	_
ODBmto	Odobesti	WS2355	45.7633	27.0558	60	Odobesti, Meteo	14/07/21	_
PLORmto	Plostina 4	WS2355	45.8512	26.6498	60	PLOR4 Meteo	01/12/01	_

The description of the data provided by the equipment that measures the radon level (Tables 4 and 5) is included in a general database (https://data.mendeley.com/datasets/28kv3gsgcz/2).

Table 4. Radon equipment used in Bisoca station (BISRAERd), produced by ALGADE (discontinued).

Equipment_AERC				
ID	**Field1**	**Field2**	**Field3**	**Field4**
1	Radon	Temperature (C)	Humidity (%)	Status
2	Bq/m3	C	%	_
3	%d	%0.1f	%d	%d
4	radon, Radon, temperature in the equipment - Temperature (C), relative humidity in the equipment - Humidity (%), Sigfox network connection status - Status.			

Table 5. Radon equipment produced by SARAD.

Equipment _RADONSCOUTp							
ID	**Field1**	**Field2**	**Field3**	**Field4**	**Field5**	**Field6**	**Field7**
1	Radon	Error	Temp	relHum	Pres	Tilt	ROI1
2	Bq/m3	%	C	%	mbar	_	cts

Preprints (www.preprints.org) | NOT PEER-REVIEWED | Posted: 23 May 2023 doi:10.20944/preprints202305.1645.v1

3	%d	%d	%0.1f	%d	%d	%d	%d
4	radon, Radon, error - Error, temperature in the equipment - Temp, relative humidity in the equipment - relHum, atmospheric pressure - Press, inclination - Tilt, region of interest 1 - ROI1.						

Besides the position of the monitoring station and the type of equipment used, its installation is also important. The only monitoring station built specifically for this purpose is at Râmnicu Vâlcea (location Electrovalcea SRL), Figure 3, RMGVdd in Tables 1 and 2. The description of Figure 3 according to the patent application 'OSIM a 2020 00500 10/08/2020' ([11]) is:

PF	**-**	**Borehole, 40m deep;**
D	-	Diameter between 300 and 500mm;
SV	-	Vibration sensor (triaxial accelerometer);
PS	-	Glass balls for fixing SV;
ST	-	Temperature sensor;
T_{PVC}	-	PVC tube;
C	-	PVC cover;
P	-	10 - 30mm gravel that ensures the diffusion of radon from the bottom of the well to the SRn radon sensor;
SRn	-	Radon sensor mounted in the CV visiting space made of reinforced concrete;
CV	-	visiting space;
CM	-	Metal cover;
PPC	-	Precursor parameters of earthquakes.

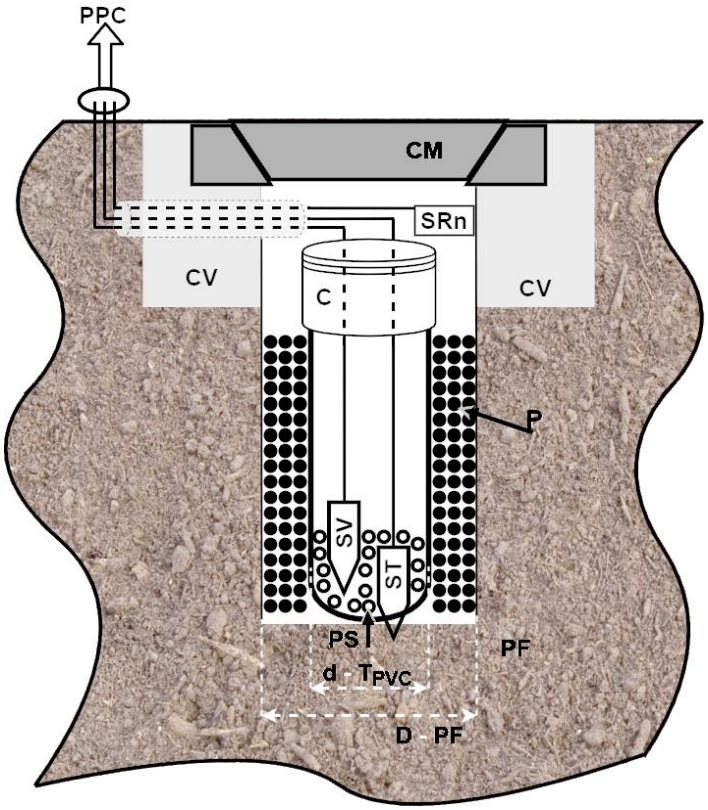

Figure 3. Installation of radon and acceleration sensors in a 40 m deep borehole [11].

This station was considered a reference because there were no seismic events in the area. Starting with 2023/02/08, over 2000 surface earthquakes occurred at an approximate distance of 80 Km in

Preprints (www.preprints.org) | NOT PEER-REVIEWED | Posted: 23 May 2023 doi:10.20944/preprints202305.1645.v1

OLTENIA – GORJ area (example in Table 7), the maximum magnitude being 5.7R. However, no radon level anomalies were recorded in RMGVdd.

3. Analysis methods and case studies

The analysis methods used are described in [2] and [3]. These were verified in relation to Vrancea seismicity and they are currently used for the analysis of the effects of climate change. Mainly the time series representing gas emissions (radon, CO_2) are integrated after the average value has been extracted, then an STA/ LTA (Short-Term Averages/ Long-Term Averages) detection algorithm type Allen ([27–29]) or 2SD (twice Standard Deviation) is applied [30]. Signal integration is done with a function that performs numerical integration from the LabVIEW library using trapezoidal rule.

An example of a case where these methods are applied is related to the sequence of surface earthquakes in the area of Râmnicu Sărat (city in Romania, Figure 5) that could have been caused by the seismic events in Turkey (2023/02/06, 7.8R and 7.5R, Figure 4) with which overlapped (Table 6).

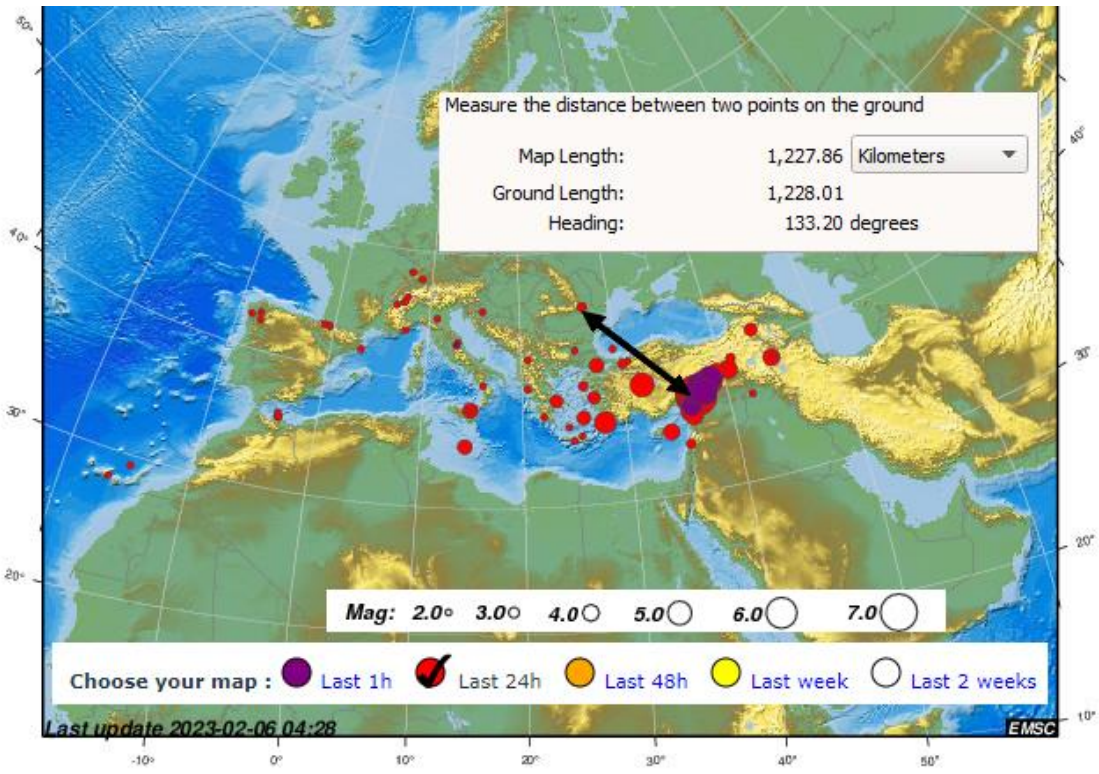

Figure 4. Superposition of the earthquake swarm in Romania with the seismic events in Turkey (2023/02/06, 7.8R and 7.5R), EMSC picture.

Preprints (www.preprints.org) | NOT PEER-REVIEWED | Posted: 23 May 2023 doi:10.20944/preprints202305.1645.v1

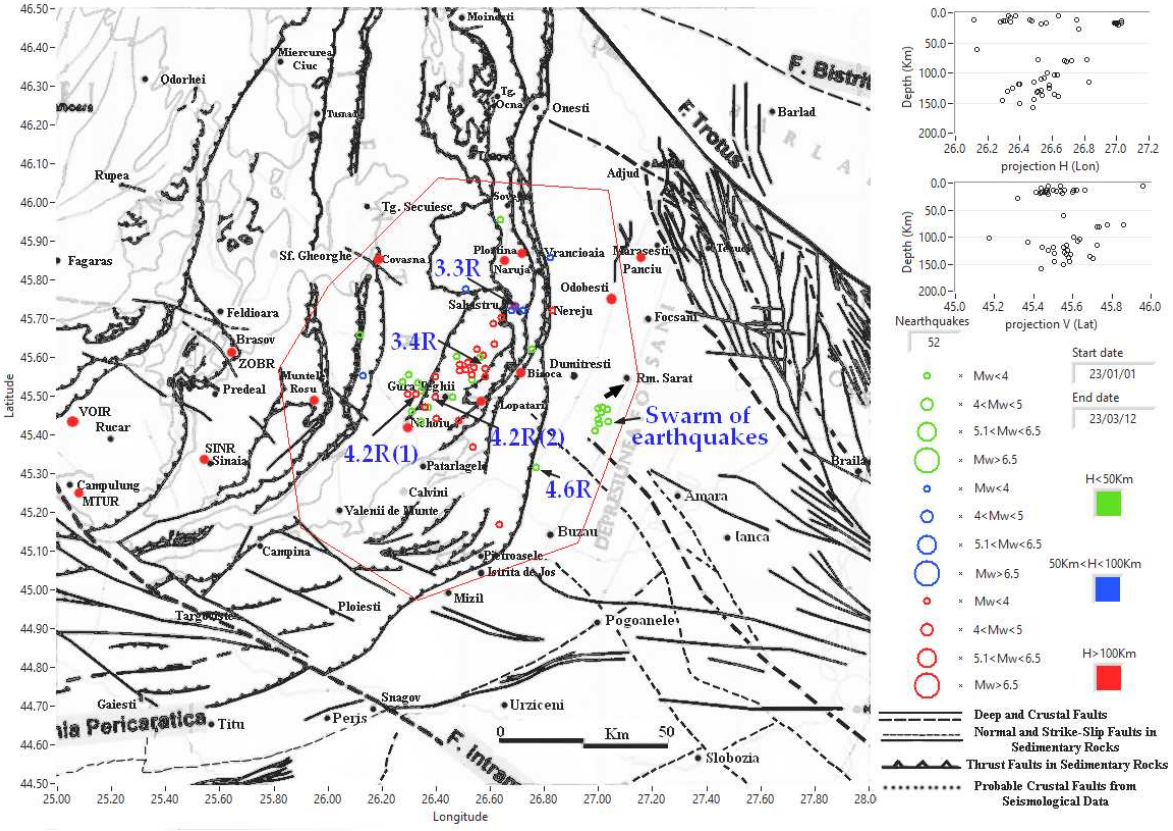

Figure 5. Vrancea seismicity and the correlation of epicenters with geological faults, 2023/01/01 - 2023/03/12, **s**warm of Râmnicu Sărat earthquakes (green circles) and 4.2R earthquakes sequence.

Table 6. Overlap of earthquakes in Turkey and Romania**,** http://www.infp.ro/.

Data (UTC)	Mag.	Reg.	h(Km)
2023/02/06, 10:51:41	5.6 ml	CENTRAL TURKEY	10km
2023/02/06, 10:24:53	7.5 ml	CENTRAL TURKEY	10km
2023/02/06, 06:55:14	5.0 ml	CENTRAL TURKEY	10km
2023/02/06, 03:26:19	2.0 ml	ZONA SEISMICA VRANCEA, BUZAU	21km
2023/02/06, 03:01:58	2.7 ml	ZONA SEISMICA VRANCEA, BUZAU	17km
2023/02/06, 02:40:31	2.1 ml	ZONA SEISMICA VRANCEA, BUZAU	13km
2023/02/06, 02:13:10	2.9 ml	ZONA SEISMICA VRANCEA, BUZAU	17km
2023/02/06, 02:09:54	2.6 ml	ZONA SEISMICA VRANCEA, BUZAU	17km
2023/02/06, 01:26:20	4.6 ml	ZONA SEISMICA VRANCEA, BUZAU	22km
2023/02/06, 01:17:36	7.8 ml	CENTRAL TURKEY	10km

Table 6 shows that the first seismic event in Turkey (2023/02/06,, 01:17:36, 7.8R) is shortly followed by the one in Romania (2023/02/06,, 01:26:20, 4.6R) at a distance of 1228 Km.

Preprints (www.preprints.org) | NOT PEER-REVIEWED | Posted: 23 May 2023 doi:10.20944/preprints202305.1645.v1

The closest radon and CO_2 monitoring stations are in Dalma (DLMdd), Bisoca (BISRAERd) and Lopatari (LOPRdd). Table 1. Applying the mentioned methods, we obtain the evolution of radon and CO_2 as in Figure 6. Only for LOPRdd we used the 2SD detection method [24], while for the others STA/ LTA. It is observed that radon and CO_2 have similar variations and those in Bisoca and Dalma are similar, unlike those in Lopatari. Also, the detections (marked with red dots) can be associated with groups of earthquakes and the seismic pause that preceded the sequence of earthquakes was longer (7 days seismic quiescence [11]). In conclusion, the first seismic event in Turkey could only have triggered what is happening anyway, the Râmnicu Sărat area being known for such behavior.

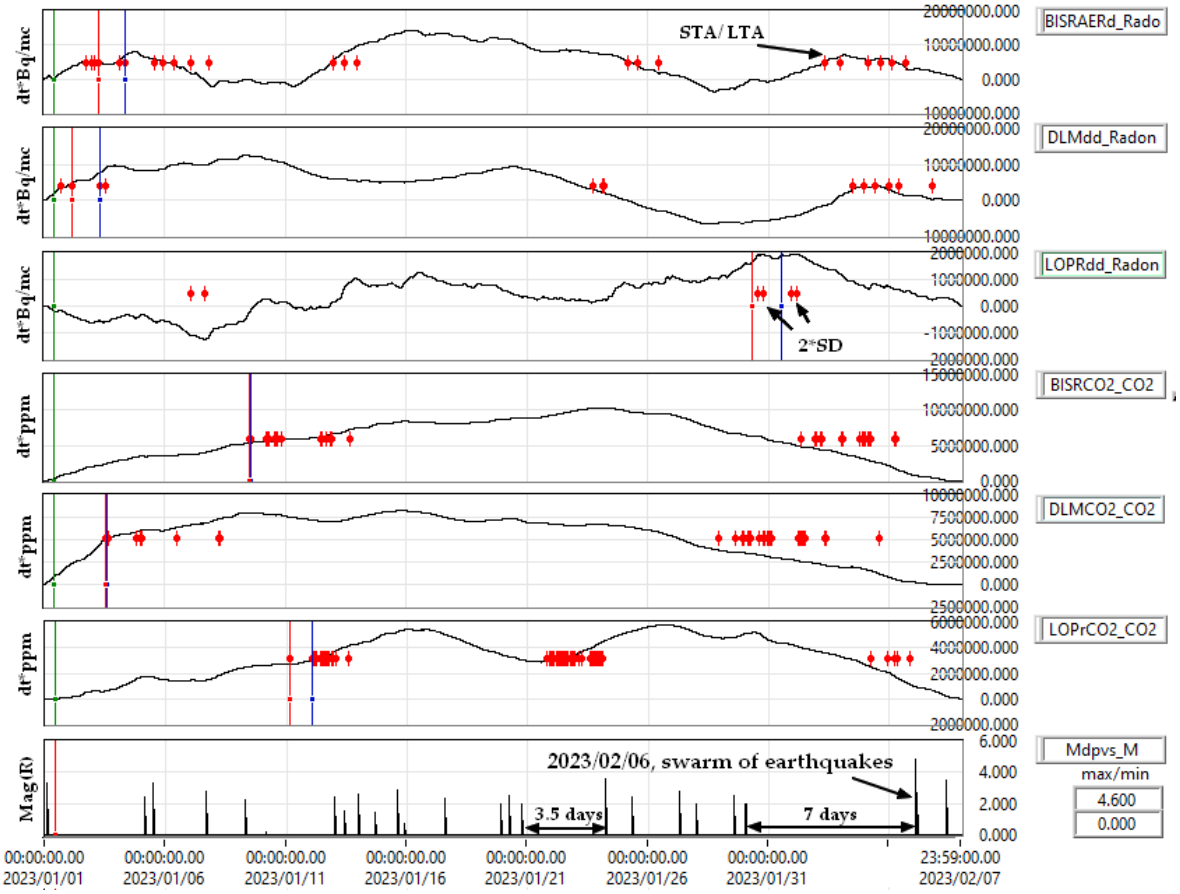

Figure 6. The evolution of radon and CO_2 preceding the earthquake sequence near Râmnicu Sărat.

Another case study is the earthquakes sequence from 2023/03/11 - 2023/03/12 in which we had two earthquakes of 4.2R accompanied by two others of 3.3R and 3.4R. These are presented in Figures 5 and 7 and Table 7.

Preprints (www.preprints.org) | NOT PEER-REVIEWED | Posted: 23 May 2023 doi:10.20944/preprints202305.1645.v1

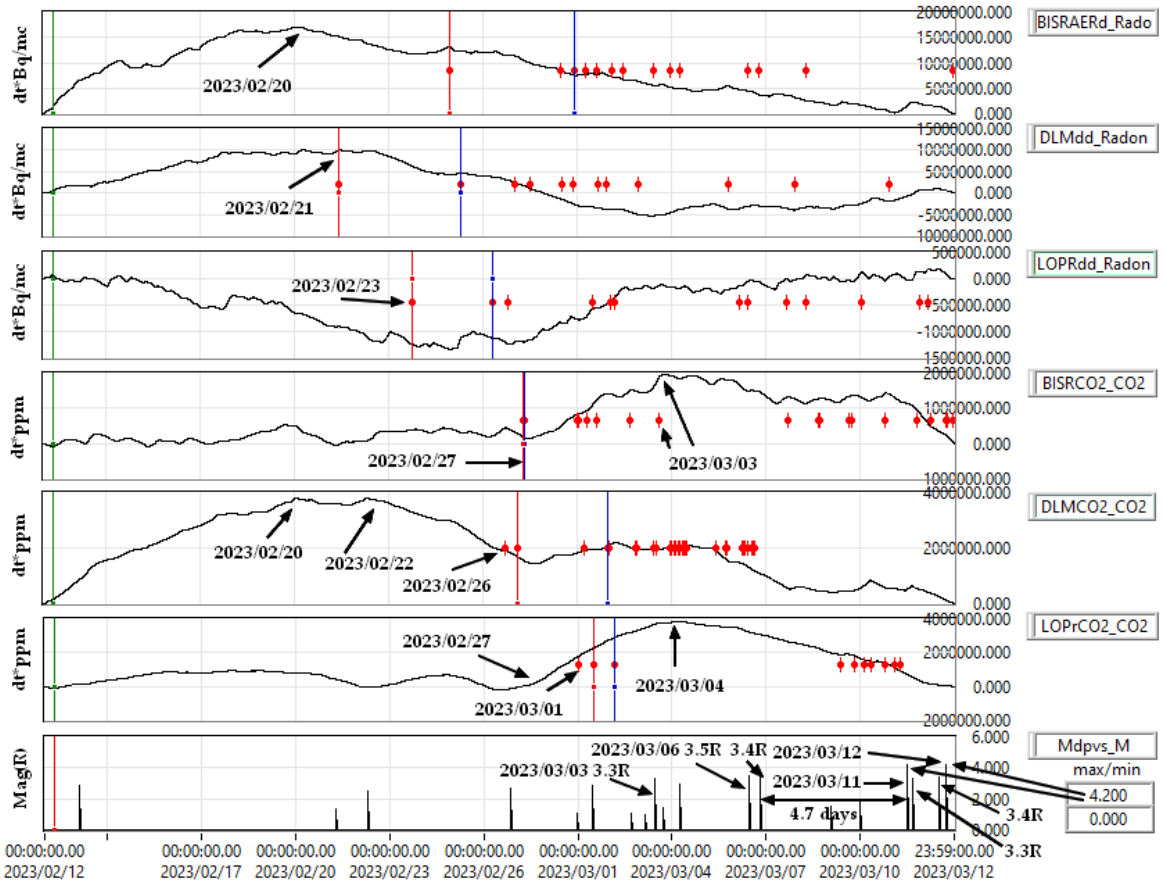

Figure 7. The evolution of radon and CO_2 for 4.2R earthquakes sequence.

Table 7. Seismic sequence in the Vrancea area, maximum M 4.2 R, swarm of earthquakes OLTENIA, GORJ.

Data (UTC)	Mag.	Reg.	h(Km)
2023/03/12, 19:12:12	2.5 ml	OLTENIA, GORJ	13km
2023/03/12, 17:44:22	**4.2 ml**	**SEISMIC AREA VRANCEA, BUZAUL**	**131km**
2023/03/12, 12:15:09	3.6 ml	OLTENIA, GORJL	16km
2023/03/12, 11:49:23	**3.4 ml**	**SEISMIC AREA VRANCEA, BUZAU**	**125km**
2023/03/11, 20:12:55	2.2 ml	OLTENIA, GORJ	15km
2023/03/11, 17:51:56	2.6 ml	OLTENIA, GORJ	14km
2023/03/11, 15:53:22	**3.3 ml**	**SEISMIC AREA VRANCEA, VRANCEAL**	**82km**
2023/03/11, 14:17:06	3.5 ml	OLTENIA, GORJL	17km
2023/03/11, 13:28:57	2.5 ml	OLTENIA, GORJ	16km
2023/03/11, 13:25:46	2.4 ml	OLTENIA, GORJ	15km
2023/03/11, 12:09:20	**4.2 ml**	**SEISMIC AREA VRANCEA, BUZAUL**	**118km**

Preprints (www.preprints.org) | NOT PEER-REVIEWED | Posted: 23 May 2023 doi:10.20944/preprints202305.1645.v1

The 4.2R earthquakes are located in the Gura Teghii seismic zone and all epicenters are on faults (Figure 5). The detections starting with 2023/02/20 in Figure 7 (red points) are of the STA/LTA type and are applied to the integrated time series. There is a similarity in time variations between radon in BISRAERd, DLMdd and carbon dioxide in DLMCO2 (maximum during 2023/02/20 followed by a decrease). Also, the evolution of radon in LOPRdd is similar to CO_2 in BISRCO2 and LOPrCO2.

We can say that the method described in [1] and [2] is also verified in this case and what matters is the grouping of earthquakes in a short period of time (1 - 2 days) even if their magnitude is not high.

The next analyzed case refers more to environmental pollution than to a relationship between gas emission and seismicity. In Table 2, the last two stations (named agigea, Agigea locality and MNGdd, locality Mangalia) refer to the results of radon monitoring at the Black Sea (their positioning is in Table 1). A large difference is observed in the level of radon caused by MNGdd, while in Agigea the radon values are normal (Table 2). However, the time periods in which the determinations were made should be noted. Those in Mangalia are recent and may be affected by the development of the city and the port. Not only the high values attract our attention, but also the way in which the gas emission varies in this location. In Figure 8 very large variations of radon that do not repeat at intervals of one day and do not depend on temperature, atmospheric pressure, precipitation or wind (EFORmt2 is a meteorological station, Table 3). Besides these, the presence of CO and the way it varies indicates a pollution that can be caused by the activity of the port, a hospital or the nearby water treatment plant. The radon measurements at the Black Sea were described in [31] where the emission of gases (radon, CO_2, methane, hydrogen sulfide) is specified and analyzed, but not in the coastal region of Romania.

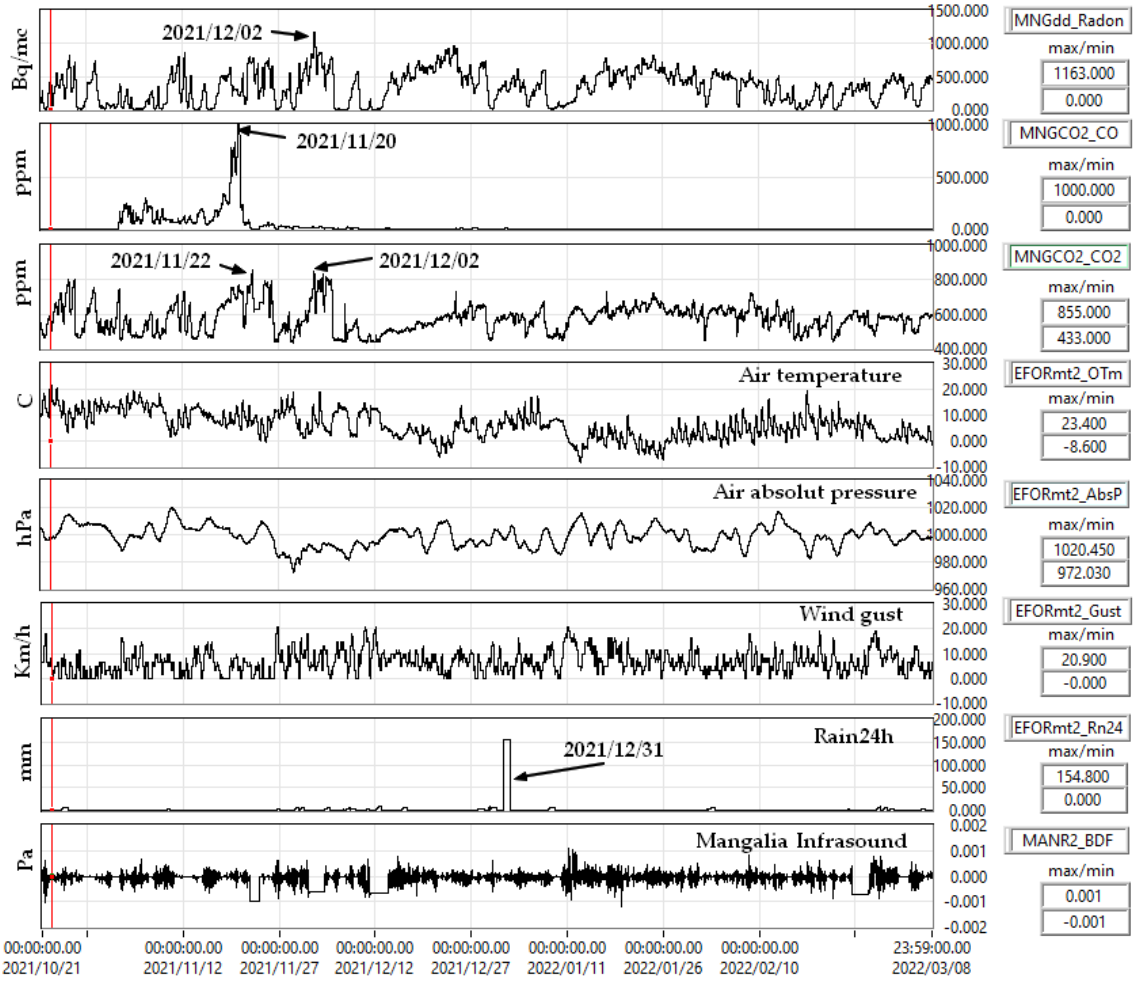

Figure 8. The case of Mangalia, the evolution of radon, CO_2 and atmospheric conditions.

Preprints (www.preprints.org) | NOT PEER-REVIEWED | Posted: 23 May 2023 doi:10.20944/preprints202305.1645.v1

Another case that draws our attention from Table 2 refers to the fact that the radon exceed the 300 Bq/mc in Surlari station (Figure 9, SURLdd), limit established by Council Directive 2013/59/EURATOM. The building in which the radon detector is located is made of brick and is located in a forest (Figure 9b).

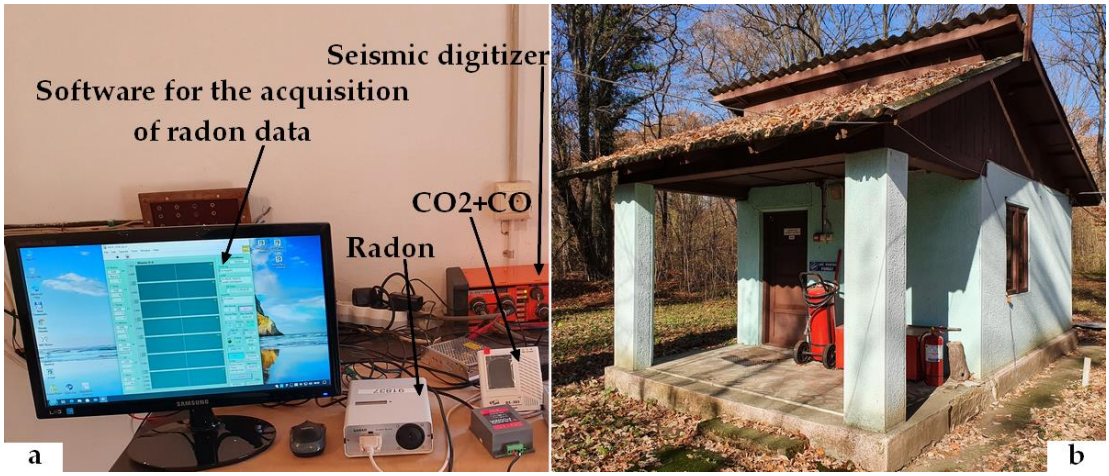

Figure 9. Surlari monitoring station: {a} Radon, CO_2 and CO equipment; (b) the location is in a forest.

The evolution of radon and CO_2, maximum and minimum values along with temperature and humidity in this location are presented in Figure 10.

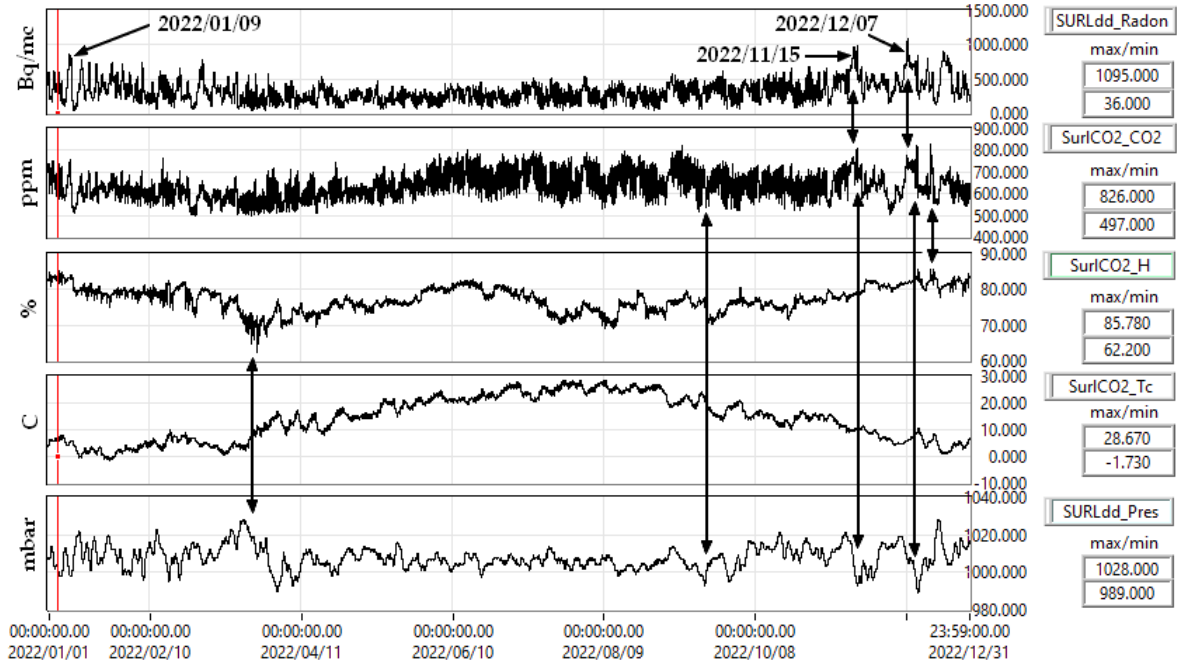

Figure 10. Radon, CO_2, temperature, air pressure in Surlari station (SURLdd).

It is observed that there is a relationship between the radon level and temperatures in the sense that during the winter the radon emission increases. The Surlari location is close to the Intramoesica fault and is characterized by surface seismicity. It is observed that there is a relationship between the radon level, temperature, humidity, and atmospheric pressure ([25,32,33]). Seasonal variation indicates an increase in radon emission in winter (lower temperatures) while CO_2 increases in summer (higher temperatures). The daily variations of radon indicate a maximum around 10 UTC hour and a minimum approximately at 19 UTC hour. After filtering with a median filter (LabVIEW library) on the time series from Figure 10 for reduce the daily variations and spikes, we applied a

Preprints (www.preprints.org) | NOT PEER-REVIEWED | Posted: 23 May 2023 doi:10.20944/preprints202305.1645.v1

cross-correlation function (LabVIEW library) and obtained the average values from Table 8 (example in Figures 11 and 12). Regardless of the chosen method, it is important that it is used under the same conditions in all the analyzed cases. So, Table 8 is relative to this method over the entire time period (one year) and allows comparative data analysis. The possible high values of radon and CO_2 levels are the relation between gas emission and vegetation ([34,35]). The operation of the equipment was checked under normal conditions and the results were satisfactory.

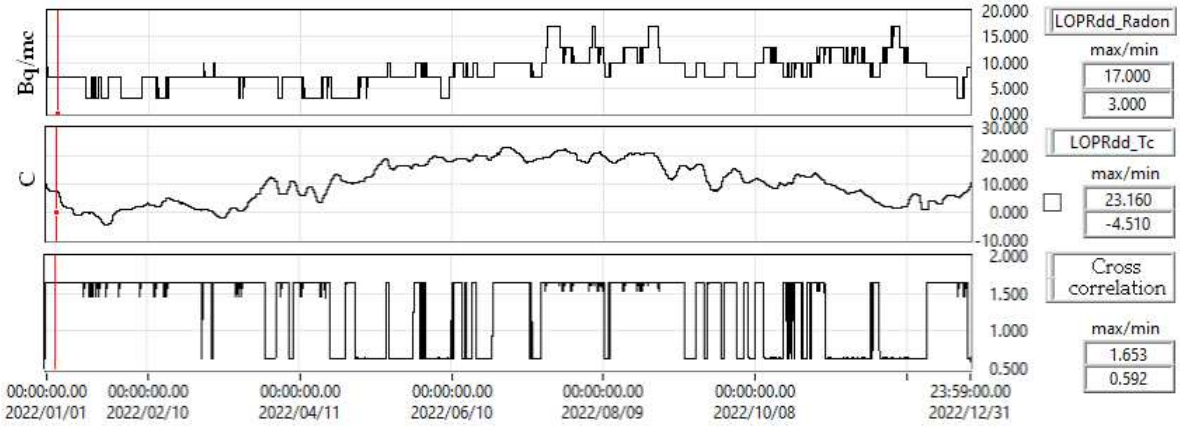

Figure 11. Cross correlation between radon and humidity in Lopatari station, 2022, 1 hour intervals.

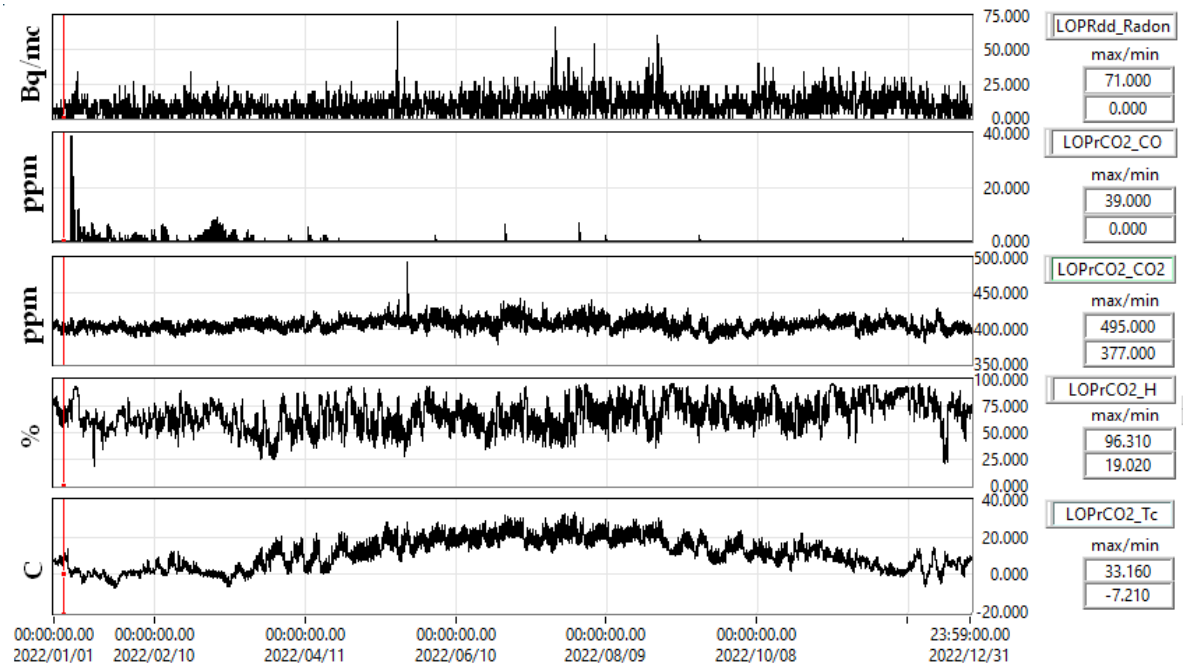

Figure 12. Gas emissions in Lopatari, 2022.

Table 8. Cross correlation coefficients.

Radon/ 2022	Station Code						
Mean Cross correlation	**SURLdd**	**LOPRdd**	**NEHRdd**	**PANCdd**	**RMGVdd**	**SAHRdd**	**BISRAERd**
CO_2	0.3354	0.2758	-0.1701	-	-	-	0.1789
Humidity	0.4430	0.3696	0.2531	0.5708	0.1814	-0.2932	0.2504
Temperature	-0.4181	0.3900	0.1370	-0.2294	0.1467	0.7436	0.4714
Atmospheric pressure	0.0797	0.2313	-0.0152	0.0088	-0.0343	-0.1636	-0.0946

Preprints (www.preprints.org) | NOT PEER-REVIEWED | Posted: 23 May 2023 doi:10.20944/preprints202305.1645.v1

Another theme is the influence of meteorological parameters on gas emissions that is generally presented in many articles ([25,36,37]). For our case study we chose the same time period (year 2022) as in Figure 10 to follow the evolution of radon and CO_2 in correlation with temperature, humidity and atmospheric pressure. Table 8 shows the correlation between radon and CO2, humidity, temperature and atmospheric pressure (the parameters measured complementary by the same equipment) for 2022 year.

We notice in Figure 10 that there are correlations over short time intervals. We redo the comparative analysis for the year 2022 but at on a sliding time window of one hour and calculate the average of the obtained coefficients (Table 9). If a positive correlation prevails, then we will have higher positive final values. But we can also have an inverse correlation (the sizes are inversely proportional) which leads to mostly negative results. The way in which the method is applied is represented in Figure 11. So, the values in Tables 9 and 10 are relative and allow an assessment of the dependence of radon on atmospheric factors.

Table 9. Cross correlation for time windows of 1 hour.

Radon/ 2022 1h	Station Code						
Mean Cross correlation	**SURLdd**	**LOPRdd**	**NEHRdd**	**PANCdd**	**RMGVdd**	**SAHRdd**	**BISRAERd**
CO_2	0.5257	0.6222	0.3742	-	-	-	0.5791
Humidity	0.6385	0.6959	0.6321	0.7216	0.5371	0.3966	0.6902
Temperature	0.3048	0.6529	0.5702	0.3742	0.5663	0.7545	0.6999
Atmospheric pressure	0.5753	0.5892	0.4674	0.5691	0.4569	0.3818	0.4807

Table 10. Vrancea seismicity for earthquakes greater than 4.5 R, 2016 - 2022.

N	Time	Ml>4.5	Depth	Longitude	Latitude	Mw	PZone
	yyyy/mm/dd	Richter	Km	Degrees	Degrees		Km
1	2016/09/23 23:11:20	5.8	92.0	26.6181	45.7148	5.52	236.8
2	2016/12/27 23:20:56	5.8	96.9	26.5987	45.7139	5.52	236.8
3	2017/02/08 15:08:21	5.0	124	26.2886	45.4791	4.6	95.3
4	2017/05/19 20:02:45	4.7	120.6	26.7581	45.7249	4.32	72.3
5	2017/08/01 10:27:52	4.6	96.6	26.4681	45.5146	4.24	66.3
6	2017/08/02 02:32:13	4.9	132.5	26.4014	45.5267	4.51	86.7
7	2018/03/14 10:24:49	4.6	139.1	26.5850	45.6759	4.24	66.3
8	2018/04/25 17:15:49	4.6	147.3	26.4216	45.6002	4.24	66.3
9	2018/10/28 00:38:11	5.8	151.3	26.3986	45.6049	5.52	236.8
10	2019/09/03 11:52:53	4.5	116.7	26.2896	45.4712	4.15	61.0
11	2020/01/31 01:26:48	5.2	120.6	26.7033	45.7106	4.80	116.4
12	2020/04/24 22:04:19	5.0	21.6	27.4651	45.8951	3.79	42.8
13	2020/06/02 11:12:58	4.5	101.2	26.5548	45.6239	4.15	61.0
14	2021/04/09 18:36:47	4.5	77.1	26.6292	45.7916	4.15	61.0
15	2021/05/25 21:30:37	4.7	130.9	26.5226	45.5321	4.32	72.3
16	2021/09/01 10:32:12	4.5	145.0	26.4474	45.6413	4.15	61.0
17	2022/11/03 04:50:26	5.3	148.8	26.5166	45.4949	4.91	129.4
18	2022/12/17 05:42:59	4.5	140.0	26.4668	45.6359	4.15	61.0

A special case in Lopatari is CO as a result of burning gases produced by live fires (Figure 12). The time series used in Tables 8 and 9 are presented in Figures 12 and 13. In general, temperature and humidity are inversely proportional (an example in Figure 12 for the Panciu station, PANCdd). This, as well as the dependence of radon on atmospheric factors, depend on the way the equipment is installed. In Table 8 it can be seen that the dependence of radon on temperature is very small in

Preprints (www.preprints.org) | NOT PEER-REVIEWED | Posted: 23 May 2023 doi:10.20944/preprints202305.1645.v1

Lopatari (LOPRdd) because the measurements are made by the same equipment (Radon Scout Plus) which is in a partially air-conditioned space. For this reason, the relationship between temperature and humidity differs from normal conditions, Figure 12 (for example in Panciu, Figure 13). A similar situation exists in Bisoca (BISRAERd).

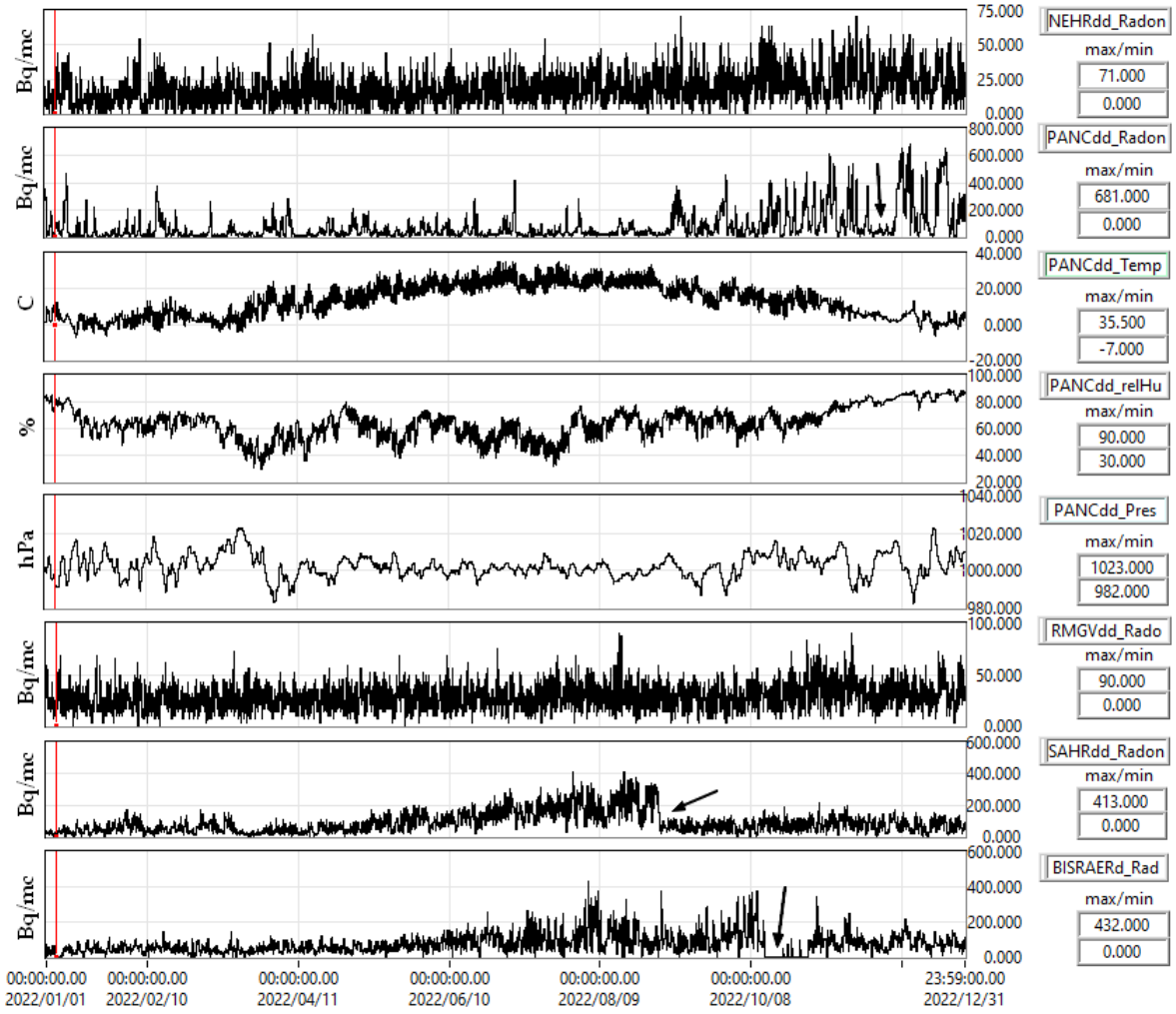

Figure 13. Dependence of radon on atmospheric factors, 2022.

Laboratory measurements of radon highlighted the same direct positive relationship between radon emission and temperature [38]. This is valid if the radon emission and its measurement are done in the same place. In our locations, the rooms where the equipment are placed are not hermetically sealed and radon can come from nearby areas as a result of air currents. From Figures 10, 12 and 13 a similar evolution of radon can be observed in LOPRdd, RMGVdd, SAHRdd and BISRAERd (higher values in summer) and for SURLdd, NEHRdd and PANCdd higher values in winter. These results are preserved if we analyze the evolution of radon over several years (Figure 14).

Preprints (www.preprints.org) | NOT PEER-REVIEWED | Posted: 23 May 2023 doi:10.20944/preprints202305.1645.v1

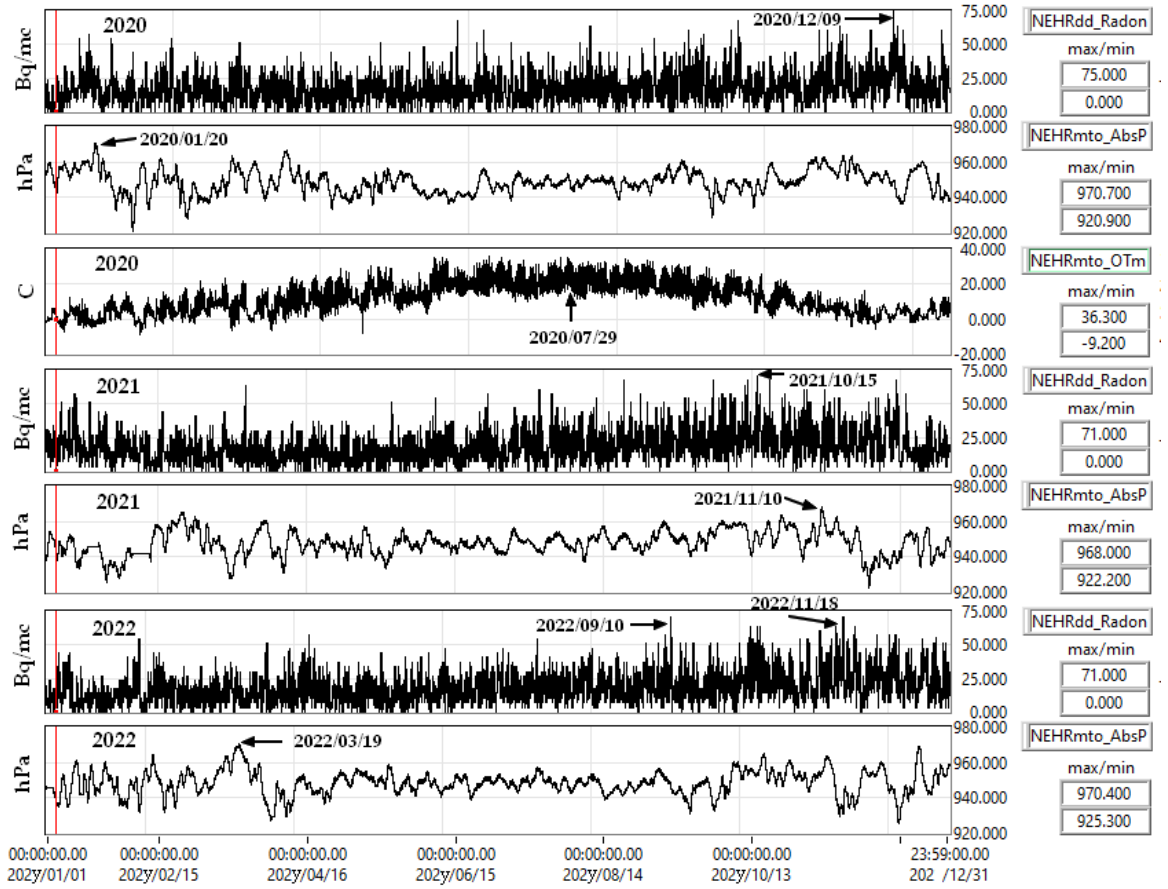

Figure 14. The annual evolution of radon in Nehoiu (NEHRdd) and environmental factors.

Next case analyzed concerns the relationship between radon emission and seismicity. We have already analyzed the Râmnicu Sărat cases (Table 6, Figure 6) and the sequence of earthquakes from 2023/03/11 - 2023/03/12 (Table 7, Figure 7). We now choose a longer period of time between 2016 and 2022 and earthquakes greater than 4.5R in the Vrancea area, Table 10. The preparation zone PZone is determined by Dobrovolsky's relation [39] depending on the magnitude. The relationship is checked experimentally using Mw. The monitoring station should be in this area to be able to assess a relationship between radon and earthquakes. Different formulas of relations between earthquake magnitude and preparation distance of different authors were mentioned by Nevinsky in [31]. In general, this condition is met in Table 10 because we chose a threshold of 4.5 R for the magnitude. The relationship between the accumulated seismic energy, the parameters a-b from Gutenberg – Richter law [12,13], seismicity and the number of earthquakes produced in a 7-day interval is presented in Figure 15.

Preprints (www.preprints.org) | NOT PEER-REVIEWED | Posted: 23 May 2023 doi:10.20944/preprints202305.1645.v1

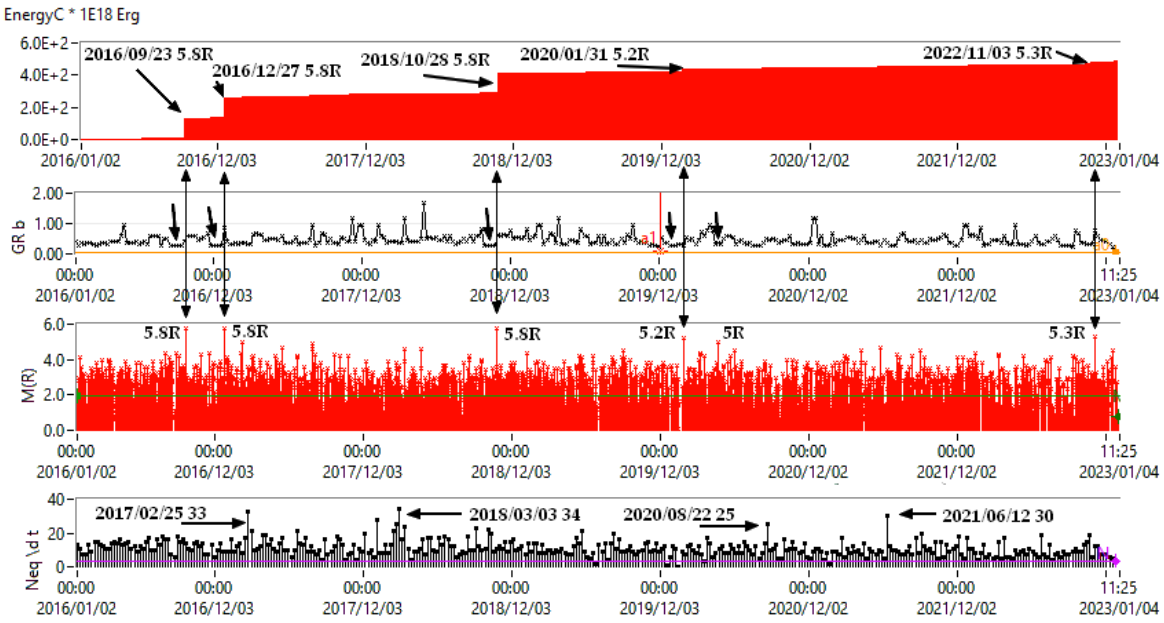

Figure 15. Cumulative seismic energy, the Gutenberg-Richter parameter 'b', seismicity and the number of earthquakes produced in a 7 interval.

From Figures 15 and 16 it can be seen that a decrease over a period of more than 18 days of the parameter 'b' from the Gutenberg-Richter law (GR_b) is followed by earthquakes with a magnitude greater than 5R (observation valid for the Vrancea area). The radon and temperature time series in Figure 16 were averaged to mitigate daily variations. We note that the maximum values of radon levels are between August and November and do not correlate with the number of earthquakes produced at 7-day intervals (Neq/dt graph). We apply a correlation function between parameter 'b' from the Gutenberg-Richter law (GR_b) and radon for the period 2016 – 2022 for the case where the depth of the hypocenter is greater than 20 km or less. Depth is important because the source of radon should be on the surface because its half-life is 3.82 days. The results are in Figure 17 and Table 11.

Preprints (www.preprints.org) | NOT PEER-REVIEWED | Posted: 23 May 2023 doi:10.20944/preprints202305.1645.v1

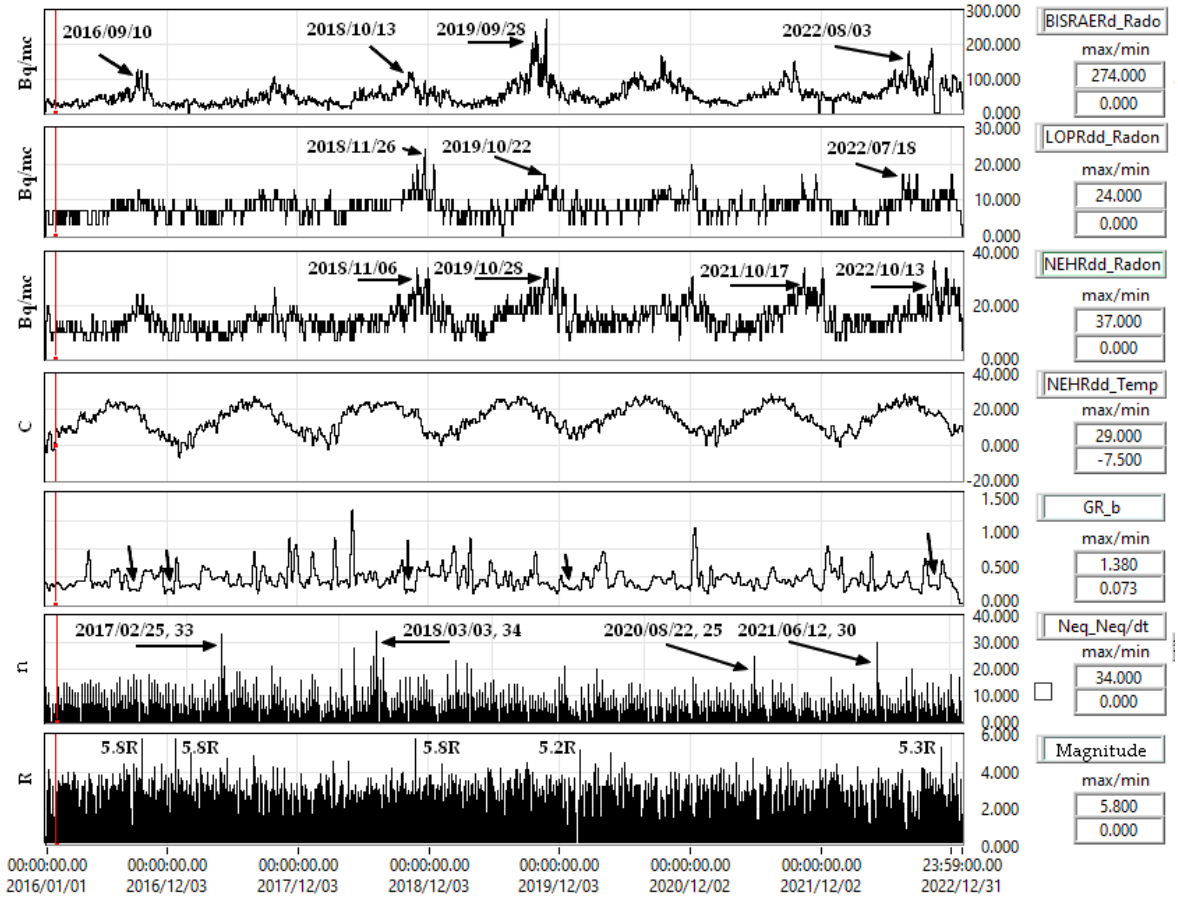

Figure 16. Evolution of radon level, temperature and seismicity in Vrancea, time windows 7 days, 2016 – 2022.

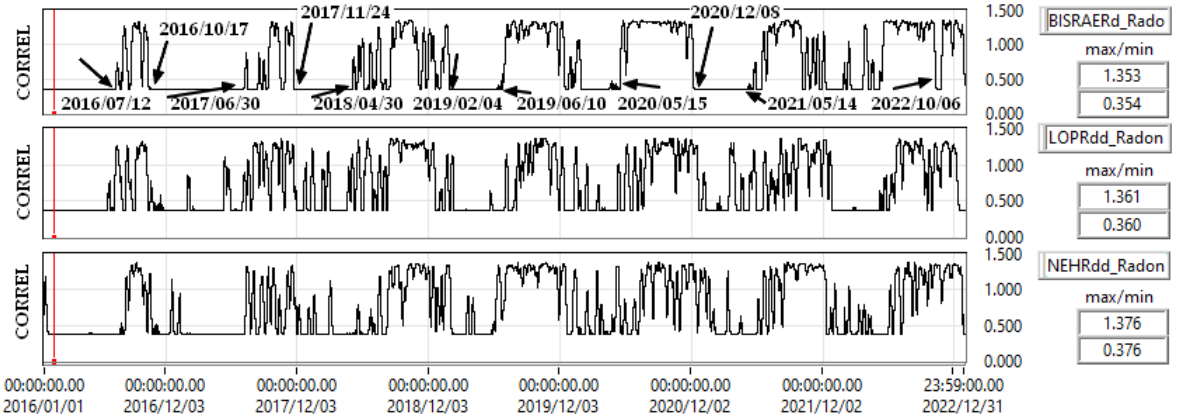

Figure 17. CORREL between Gr_b (Gutenberg – Richter law) and radon BISRAERs, LOPRdd, NEHERdd.

Table 11. Correlation factor between 'b' parameter and radon in BISRAERd, LOPRdd, NEHERdd, 2016 – 2022, time windows of 7 days.

Station, 2016 - 2022	**Mean**	Standard Deviation	Mean	Standard Deviation
	H>20 Km		H<20 Km	
BISRAERd	0.3541	30.9621	0.3562	30.9617
LOPRdd	0.3707	2.7410	0.3703	2.7410
NEHRdd	0.3766	5.1496	0.3751	5.1495

Preprints (www.preprints.org) | NOT PEER-REVIEWED | Posted: 23 May 2023 doi:10.20944/preprints202305.1645.v1

Correlation of 'b' parameters between crustal and deep seismicity for Vrancea using a sliding time window of 7 days is in Figure 18 where Mean = 0.8767 and SD = 0.4508.

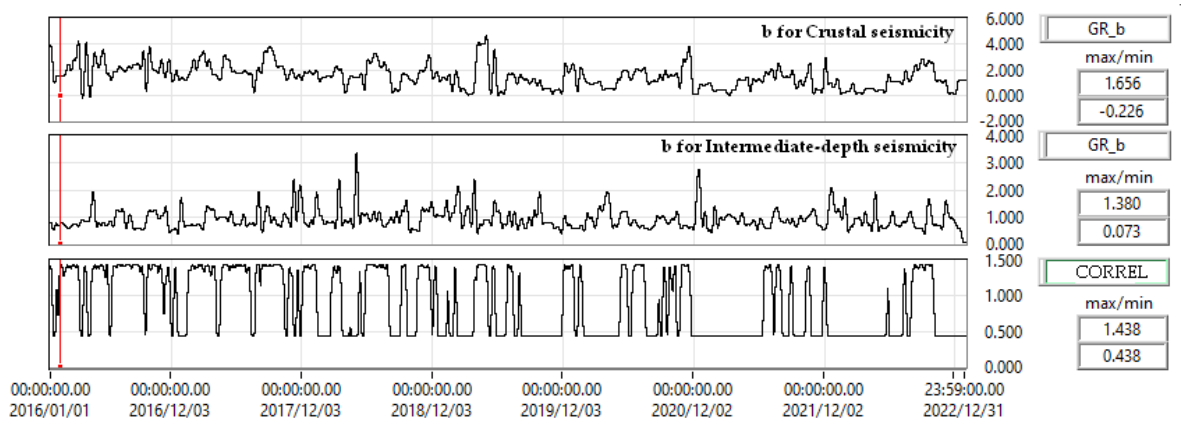

Figure 18. Correlation between b from Gutenberg – Richter law for Vrancea crustal and deep seismicity.

Integrating the time series from Figure 16 we obtain the radon variations from Figure 19. We observe a continuous increase in radon level along with the temperature, which we can interpret as an effect of climate change.

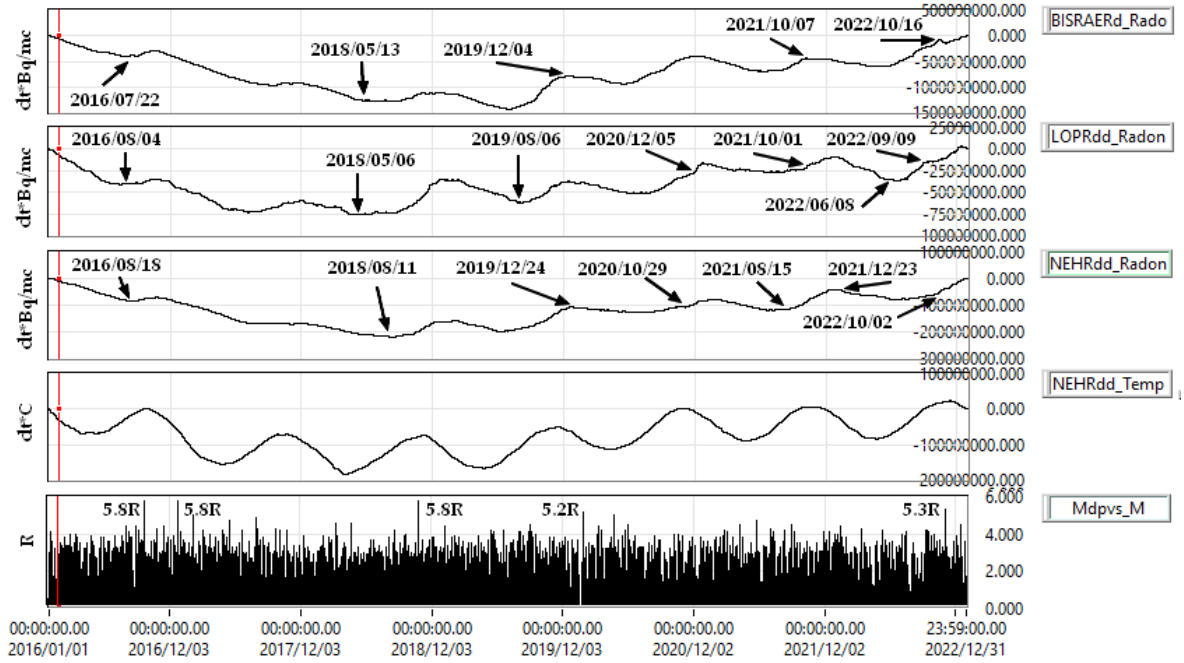

Figure 19. Annual variations of radon integrated and Vrancea seismicity, 2016 – 2022.

4. Conclusions

From the data presented, it is not possible to establish an exact relationship between the anomalies of radon emissions and seismicity, but evaluations can be made that can be completed with forecasts. Radon level recording depends on environmental factors, location and installation area. For this reason, the results presented in different articles for different domains may be different. An example has already been mentioned regarding the evolution of radon in LOPRdd, RMGVdd, SAHRdd and BISRAERd (higher values in summer) and for SURLdd, NEHRdd and PANCdd higher values in winter (Figure 10, 12 and 13). We have chosen monitoring positions near geological faults, but it is not enough because they may not be active for gas emission. The investigation area was Vrancea (the curvature area of the Carpathian Mountains), which is characterized by deep

earthquakes (Table 10). Table 11 shows that the mean value of the correlation factors determined in a 7-day sliding window and the corresponding SD are close in value for surface and depth earthquakes (correlation between 'b' parameters in Figure 18). These determinations (Table 11) depend a lot on the calculation method and the way the time series were filtered. We apply first a median filter (LabVIEW library) on the time series from Figure 10 for reduce the daily variations and spikes, next we used a cross-correlation function (LabVIEW library) and obtained the average values and SD. For this reason, it is important to use the same method for all determinations and the analysis of the results to be comparative.

The radon level depends on the tectonic stress that induces a deformation of the rocks ([38,40–42]), which in turn depends on the environmental factors. For this reason, the use of a trigger threshold per level for anomaly detection is not possible, but a real-time OEF (Operational Earthquake Forecasting) can be implemented like in [2]. There will always be a degree of uncertainty because the emission of radon and gases in general depends on many factors. For this reason, a validation with other parameters is necessary. In presenting the link between the radon level and seismicity, we used the parameters a - b from the Gutenberg-Richter law (Figure 15). We observe that a decrease over a period longer than 18 days of the parameter 'b' from the Gutenberg-Richter law (GR_b) is followed by earthquakes with a magnitude greater than 5R (Figures 15 and 16) for the Vrancea area. For this reason, there is no general method and an implementation of an OEF must take into account the particularities of the monitoring area ([4–8]). In our case, the Vrancea area is unique in Europe due to its geological structure and its deep earthquakes.

Author Contributions: Conceptualization, V.-E.T.; methodology, V.-E.T. and I.-A.M.; software, V.-E.T.; validation, A.M, N B-B and C.I.; formal analysis, I.-A.M and I.L.; investigation, V.-E.T. and I.-A.M.; writing—original draft preparation, V.-E.T. and N B-B; correspondent, V.-E.T.; supervision, N B-B. All authors have read and agreed to the published version of the manuscript.

Funding: This work was carried out within Nucleu Program project no PN23360201.

Data Availability Statement: An example of the data is archived at https://data.mendeley.com/datasets/28kv3gsgcz, Published: 27 September 2022|Version 2|DOI:10.17632/28kv3gsgcz.2.

Acknowledgments: This paper was carried out within Nucleu Program SOL4RISC, supported by MCI, project no PN23360201 and AFROS Project PN-III-P4-ID-PCE-2020-1361, supported by UEFISCDI.

Conflicts of Interest: The authors declare no conflict of interest.

References

1. Toader VE, Moldovan IA, Marmureanu A, Dutta PK, Partheniu R, Nastase E. Monitoring of radon and air ionization in a seismic area. *Rom Reports Phys*. 2017;69(3):842013.
2. Toader VE, Nicolae V, Moldovan IA, Ionescu C, Marmureanu A. Monitoring of Gas Emissions in Light of an OEF Application. *Atmosphere (Basel)*. 2020;12(1):26. doi:10.3390/atmos12010026
3. Toader VE, Mihai A, Moldovan IA, Ionescu C, Marmureanu A, Lingvay I. Implementation of a radon monitoring network in a seismic area. *Atmosphere (Basel)*. 2021;12(8):1-14. doi:10.3390/atmos12081041
4. Omi T, Ogata Y, Shiomi K, Enescu B, Sawazaki K, Aihara K. Implementation of a Real-Time System for Automatic Aftershock Forecasting in Japan. *Seismol Res Lett*. 2019;90(1):242-250. doi:10.1785/0220180213
5. Toader, VE.; Moldovan, I.A; Mihai, A. Forecast Earthquake Using Acoustic Emission. In: *International Multidisciplinary Scientific GeoConference Surveying Geology and Mining Ecology Management, SGEM*. Vol 19. ; 2019:803-811. doi:10.5593/sgem2019/1.1/S05.100
6. Kachakhidze-Murphy N, Kachakhidze M, Biagi PF. Earthquake Forecasting Possible Methodology. *GESJ Phys*. 2016;1(15):102-111. http://gesj.internet-academy.org.ge/download.php?id=2790.pdf&t=1
7. Zechar JD, Marzocchi W, Wiemer S. Operational earthquake forecasting in Europe: progress, despite challenges. *Bull Earthq Eng*. 2016;14(9):2459-2469. doi:10.1007/s10518-016-9930-7
8. Thomas H., Yun-Tai Chen, Paolo Gasparini, et al. OPERATIONAL EARTHQUAKE FORECASTING. State of Knowledge and Guidelines for Utilization. *Ann Geophys*. 2011;54(4). doi:10.4401/ag-5350

9. Jordan TH, Marzocchi W, Michael AJ, Gerstenberger MC. Operational earthquake forecasting can enhance earthquake preparedness. *Ann Geophys*. 2011;54(4):315-391. doi:10.4401/ag-5350
10. Victorin Toader, Iren-Adelina Moldovan, Constantin Ionescu AM. ULF RADIO MONITORING NETWORK IN A SEISMIC AREA. In: *EGU General Assembly Conference*. Geophysical Research Abstracts; 2017:18037.
11. Ciogescu Ovidiu, Lingvay Daniel, Șchiopu Mihaela, Lingvay Iosif. Toader Victorin Emilian, Ionescu Constantin, Marmureanu Alexandru MA. Complex system for prediction, warning of seismic movements and fire prevention following damage to gas installations caused by major earthquakes. In: BOPI patent application 02/2021; a 2020 00500/10-08-2020, ed. *OSIM*. Vol 2. Directorat. ; 2021:35.
12. Nava FA, Márquez-Ramírez VH, Zúñiga FR, Lomnitz C. Gutenberg–Richter b-value determination and large-magnitudes sampling. *Nat Hazards*. 2017;87(1). doi:10.1007/s11069-017-2750-5
13. Toader VE, Popescu IM, Moldovan IA, Constantin I. Vrancea seismicity analysis based on cumulative seismic energy. *UPB Sci Bull Ser A Appl Math Phys*. 2015;77(2):297-308.
14. D'Incecco S, Petraki E, Priniotakis G, Papoutsidakis M, Yannakopoulos P, Nikolopoulos D. CO2 and Radon Emissions as Precursors of Seismic Activity. *Earth Syst Environ*. 2021;5(3):655-666. doi:10.1007/s41748-021-00229-2
15. Zafrir H, Barbosa S, Levintal E, Weisbrod N, Ben Horin Y, Zalevsky Z. The Impact of Atmospheric and Tectonic Constraints on Radon-222 and Carbon Dioxide Flow in Geological Porous Media - A Dozen-Year Research Summary. *Front Earth Sci*. 2020;8(October):1-28. doi:10.3389/feart.2020.559298
16. Chen Z, Li Y, Liu Z, Wang J, Zhou X, Du J. Radon emission from soil gases in the active fault zones in the Capital of China and its environmental effects. *Sci Rep*. 2018;8(1):16772. doi:10.1038/s41598-018-35262-1
17. Khan MA, Khattak NU, Hanif M. Radon emission along faults: a case study from district Karak, Sub-Himalayas, Pakistan. *J Radioanal Nucl Chem*. 2022;331(5):1995-2003. doi:10.1007/s10967-022-08283-4
18. Ioannides K, Papachristodoulou C, Stamoulis K, et al. Soil gas radon: a tool for exploring active fault zones. *Appl Radiat Isot*. 2003;59(2-3):205-213. doi:10.1016/S0969-8043(03)00164-7
19. Xuan PT, Duong NA, Chinh V Van, Dang PT, Qua NX, Pho N Van. Soil Gas Radon Measurement for Identifying Active Faults in Thua Thien Hue (Vietnam). *J Geosci Environ Prot*. 2020;08(07):44-64. doi:10.4236/gep.2020.87003
20. Haquin G, Zafrir H, Ilzycer D, Weisbrod N. Effect of atmospheric temperature on underground radon: A laboratory experiment. *J Environ Radioact*. 2022;253-254:106992. doi:10.1016/j.jenvrad.2022.106992
21. Kulali F, Akkurt I, Özgür N. The Effect of Meteorological Parameters on Radon Concentration in Soil Gas. *Acta Phys Pol A*. 2017;132(3-II):999-1001. doi:10.12693/APhysPolA.132.999
22. Ivanova K, Stojanovska Z, Djunakova D, Djounova J. Analysis of the spatial distribution of the indoor radon concentration in school's buildings in Plovdiv province, Bulgaria. *Build Environ*. 2021;204:108122. doi:10.1016/j.buildenv.2021.108122
23. Bem H, Janiak S, Przybył B. Survey of indoor radon (Rn-222) entry and concentrations in different types of building in Kalisz, Poland. *J Radioanal Nucl Chem*. 2020;326(2):1299-1306. doi:10.1007/s10967-020-07394-0
24. Al-Hilal M, Abdul-Wahed MK. Soil gas radon measurements for investigating the actual status of seismic quiescence along the bounding fault of the Ghab pull-apart basin in western Syria. *Geofis Int*. 2018;57(3):177-187.
25. Ptiček Siročić A, Kovač S, Stanko D, Pejak I. Dependence of concentration of radon on environmental parameters. *Environ Eng*. 2021;8(1-2):17-25. doi:10.37023/ee.8.1-2.3
26. Shahrokhi A, Burghele BD, Fábián F, Kovács T. New study on the correlation between carbon dioxide concentration in the environment and radon monitor devices. *J Environ Radioact*. 2015;150:57-61. doi:10.1016/j.jenvrad.2015.07.028
27. Allen VREX. AUTOMATIC EARTHQUAKE RECOGNITION AND TIMING FROM Single Traces. *Bull Seismol Soc Americ*. 1978;68(5):1521-1532.
28. Allen R. Automatic phase pickers: Their present use and future prospects. *Bull Seismol Soc Am | Geosci*. 1982;72(6B):225–S242. Accessed April 28, 2020. https://pubs.geoscienceworld.org/ssa/bssa/article-abstract/72/6B/S225/102172/Automatic-phase-pickers-Their-present-use-and?redirectedFrom=fulltext
29. Jones JP, Van Der Baan M. Adaptive STA–LTA with outlier statistics. *Bull Seismol Soc Am*. 2015;105(3):1606-1618. doi:10.1785/0120140203

30. Al-Hilal M, Abdul-Wahed MK. Soil gas radon measurements for investigating the actual status of seismic quiescence along the bounding fault of the Ghab pull-apart basin in western Syria. *Geofis Int*. 2018;57(3):177-187.
31. Nevinsky I, Tsvetkova T, Dogru M, et al. Results of the simultaneous measurements of radon around the Black Sea for seismological applications. *J Environ Radioact*. 2018;192(June):48-66. doi:10.1016/j.jenvrad.2018.05.019
32. Xie D, Liao M, Kearfott KJ. Influence of environmental factors on indoor radon concentration levels in the basement and ground floor of a building – A case study. *Radiat Meas*. 2015;82:52-58. doi:10.1016/j.radmeas.2015.08.008
33. Taşköprü C, İçhedef M, Saç MM. Diurnal, monthly, and seasonal variations of indoor radon concentrations concerning meteorological parameters. *Environ Monit Assess*. 2023;195(1):25. doi:10.1007/s10661-022-10596-6
34. Megonigal JP, Brewer PE, Knee KL. Radon as a natural tracer of gas transport through trees. *New Phytol*. 2020;225(4):1470-1475. doi:10.1111/nph.16292
35. Jayaratne ER, Ling X, Morawska L. Role of Vegetation in Enhancing Radon Concentration and Ion Production in the Atmosphere. *Environ Sci Technol*. 2011;45(15):6350-6355. doi:10.1021/es201152g
36. Aquilina N, Fenech S. The Influence of Meteorological Parameters on Indoor and Outdoor Radon Concentrations: A Preliminary Case Study. *J Environ Pollut Control*. 2019;2(1):107. www.annexpublishers.com
37. Sundal AV, Valen V, Soldal O, Strand T. The influence of meteorological parameters on soil radon levels in permeable glacial sediments. *Sci Total Environ*. 2008;389(2-3):418-428. doi:10.1016/j.scitotenv.2007.09.001
38. Tuccimei P, Mollo S, Soligo M, Scarlato P, Castelluccio M. Real-time setup to measure radon emission during rock deformation: implications for geochemical surveillance. *Geosci Instrumentation, Methods Data Syst*. 2015;4(1):111-119. doi:10.5194/gi-4-111-2015
39. Dobrovolsky IP, Zubkov SI, Miachkin VI. Estimation of the size of earthquake preparation zones. *Pure Appl Geophys PAGEOPH*. 1979;117(5):1025-1044. doi:10.1007/BF00876083
40. S.J. Bauer, W.P. Gardner HL. Real Time Degassing of Rock during Deformation. In: *50th US Rock Mechanics / Geomechanics Symposium Held in Houston, TX, USA*. ; 2016:1-7. file:///C:/Users/C57.DESKTOP-ML0C8QK.000/Downloads/Bauer et al.%252c2016_ARMA.pdf
41. Ambrosino F, Thinová L, Briestenský M, Giudicepietro F, Roca V, Sabbarese C. Analysis of geophysical and meteorological parameters influencing 222Rn activity concentration in Mladeč caves (Czech Republic) and in soils of Phlegrean Fields caldera (Italy). *Appl Radiat Isot*. 2020;160. doi:10.1016/j.apradiso.2020.109140
42. Morales-Simfors N, Wyss RA, Bundschuh J. Recent progress in radon-based monitoring as seismic and volcanic precursor: A critical review. *Crit Rev Environ Sci Technol*. 2020;50(10):979-1012. doi:10.1080/10643389.2019.1642833